Evaluation of Fracture Toughness of Composite Armor Substructures

M. Bilal Khan
School of Chemical and Materials Engineering
National University of Science and Technology, Islamabad, Pakistan.
bilalkhan-ccems@nust.edu.pk

Abstract

The fracture toughness of a series of passive armor candidate substructures has been evaluated using impact testing with special reference to interleaving viscoelastic layers fabricated in-house. A segmented polyurethane (PU) elastomer, its cross-linked counterpart and its glass fiber composite, two forms of granite, Mn-steel and the titanium (Ti) alloy, Ti-6Al-4V were tested. The PU composite exhibited the highest impact strength (IS) followed by Ti-alloy, which showed inter-crystalline, cup and cone fracture typical of highly ductile materials. Viscoelastic PU exhibited maximum energy absorption without being fractured. When used in conjunction with ductile materials, the PU augments the IS, but not so well in league with the brittle ones. The significant superior energy absorption by PU is analyzed and explained in terms of the nanostructures, attenuated total reflection infrared spectroscopy (ATR-IR) and dynamic mechanical thermal analysis (DMTA) of the polymer.

Keywords: Segmented Polyurethane, Nano-structures, Fracture Toughness, Viscoelastic Interlayers

Introduction

Composite armor is employed as protective shield to safeguard high value equipment against damage from projectile impact. The composite is a laminated structure composed of several material layers of varying thickness to absorb and dissipate input kinetic energy in the 1.70-3000 kJ range, which depends on the type of impinging projectile. The first European Conference on Composite Materials records the performance of a host of composites against impact by low and high velocity projectiles [1, 2]. In the beginning attention was focused onto such materials that must have impact resistance properties. Among these, Mn-steel was the mainstay material used to improve the survivability of the impacted structure. However, the added weight penalty owing to the high density of Mn-steel add-on armor is considered as a negative baggage in regard to the mobility of the retrofitted structure. Therefore, attention is being focused to develop materials that must be light in weight, low cost, and must also meet the impact threat scenario.

The recent revolution in advanced materials has led to the development of such materials. Polymer composites possessing high strength to weight ratios and being cost effective are attractive candidates for this demanding application. Composites based on polymers do have the ability to resist impact as they dissipate energy in the viscoelastic matrix and also absorb energy over a large surface being created as a result of delamination of the substructure. Currently there is increasing interest in the energy absorption by viscoelastic elastomers, embedded as interleaving layers in the armor kit. The role of these elastomeric interlayers on the performance of the fabricated armor is not well understood. Ideally such layers should provide energy absorption even at low temperature ambient and, if their dynamic properties are appropriately tuned, under high strain rates prevalent during impact.

Polyurethane (PU) formed by the polyaddition reaction of hydroxyl (-OH) containing prepolymer chains and diisocynates (-NCO) provides a prospective choice in this application. It is a multiphase material composed of hard (-NCO) and soft (-OH) segments. The OH differs in its backbone character. It could be polyether, polyester, or a polybutadiene structure; the type of isocyanate (-NCO) chosen depends on the degree of its reactivity [3].

The hard blocks in the PU mass are elastic, while the soft blocks are viscous in nature. In a segmented PU these are micro-phase segregated. Together they provide a viscoelastic character to the material [4]. Externally applied stress is partly recovered and partly converted into heat via viscous dissipation. The described behavior closely mimics the spring-dashpot system used as shock absorbers in automobiles. The spring (hard blocks) provides the elastic recovery, while the viscous fluid in the dashpot (soft block) absorbs and dissipates the shock into heat. PU may be filled or foamed to give a wide variety of products ranging from automobile fenders to energetic composites to viscous dampeners.

The paper compares the impact behavior of cross-linked and segmented PU with Mn-steel, a granite material and ductile titanium alloy (Ti-6Al-4V). Granite is employed to simulate the ceramic faceplate normally encountered in armor structures. Titanium and its alloys have attractive engineering properties. They are about 40 % lighter than steel and 60 % heavier than Aluminum. The combination of moderate weight and high strength gives titanium alloys the highest strength to weight ratio of any structural material. Intensive Charpy impact testing of un-notched specimens reveals that segmented PU and its glass-reinforced composite are promising candidates for replacing high fracture toughness Mn-steel in this important application, with the attendant weight saving. In

case of laminates, as apposed to the ductile backing, the PU does not complement fracture energy when used in conjunction with brittle materials like granite. Strikingly, PU when used as a stand-alone material surpasses the impact strength (IS) of all materials tested, including the otherwise costly titanium alloy. This behavior is corroborated by the high loss modulus of segmented PU in spite of its relatively rigid structure. Unique toughening mechanisms for this improvement are investigated and discussed in terms of the nanostructure of the PU polymer.

Materials

Impact test specimens, Fig.1, belonged to the following four classes, (a) conventional Mn-steel, (b) two categories of granite were chosen, namely, grey and black granite, to represent high IS refractory materials supplied by the small industries corporation, ISB (c) titanium alloy Ti-6Al-4V, supplied by Orthocare, LHR, Pak. Its choice was dictated by the moderate yield strength (9.25 GPa) and elongation (15 %) values, characteristic of ductile materials [5]. Typical applications include aircraft turbines and ordnance equipment, (d) A PU fabricated from diethylene glycol adipate polyester with a molecular weight of c. 2000 and Isonate 143L, a methylene diphenyl diisocyanate (MDI) of equivalent weight c. 143. The MDI/polyester was mixed in the 1:5 weight ratios in a planetary processor, followed by casting and curing of the coupons in a conventional oven at 60°C for several hours. 1-4, butane diol supplied by Aldrich was used as the chain extender in a proportion to yield a total hard segment (MDI plus diol) of 50 % by weight of the fabricated PU. The structures of the monomeric unit of soft segment and the MDI hard segment were reported in an earlier publication [6], (e) for comparison sake, a conventional cross-linked PU fabricated along the lines of the segmented PU, and possessing a similar modulus obtained by adjusting the cross-link density through incorporation of hexane triol, (f) a PU composite employed by the Toyota Motor Company, as a generic hammer-milled glass fiber-reinforced PU in automobile fenders. The glass fiber helps to decrease the thermal expansion mismatch between the PU composite and the steel mounting, apart from augmenting the impact strength of the composite.

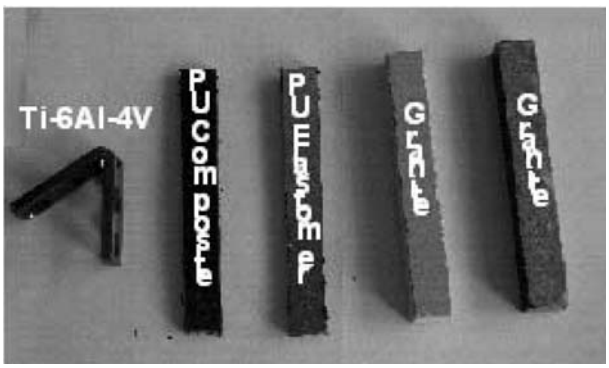

Fig. 1. Photograph of the specimens subjected to impact testing

Characterization (ATR-IR)

The fabricated PU being insoluble, solid spectroscopy was adopted. A Perkin Elmer infrared spectrometer was used with an attenuated total reflection attachment. The specimen to be examined was pressed against KRS-5 crystal and the whole assembly was tightly confined between two parallel stainless steel plates of 50 mm x 30 mm size. The IR absorption peaks obtained were examined for the various functional groups of interest. In this study three critical assignments were made: the -NH stretching vibration in the 3400 cm^{-1} region, the CH_2 stretching frequency at c.2900 cm^{-1} and the urethane carbonyl (C=O) peak in the 1700 cm^{-1} region. The depth of the sampling of the IR beam, d_p, is calculated from the following relation [7]:

$$d_p = \lambda/2\pi\eta_1(\sin^2\theta \ \eta^2_{12})^2 \quad (1)$$

Where η_1 is the refractive index of the KRS-5 (2.37) and $\eta_{12} = \eta_2/\eta_1$, η_2 being the refractive index of the PU (~ 1.25). θ is the effective incidence angle (45° in the present case). The penetration depth for the range of critical frequencies encountered lay in the 1-2 μm range.

Impact-testing

Charpy impact testing was conducted using the Brooks pendulum impact-testing machine (Brooks Inspection Equipment, U.K.). The specimen geometry is depicted in Fig.2, which corresponds to the Mode I crack propagation as indicated in Fig.3, which basically shows the three ways the forces can act and the kind of fracture they cause. In this test, pendulum release corresponds to an angle of drop of 140°. The pendulum weighing 21 kg strikes the specimen placed in the groove at an effective rate of 5.35 m/s. The electronic dial provides the impact energy dissipated in joules. Maximum rated input energy of the pendulum is 300 joules. The equipment was calibrated using standard steel notch bars supplied by the manufacturer.

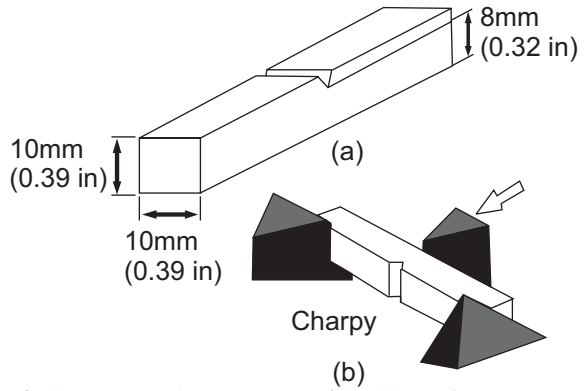

Fig. 2. Geometry and arrangement of the Charpy impact test

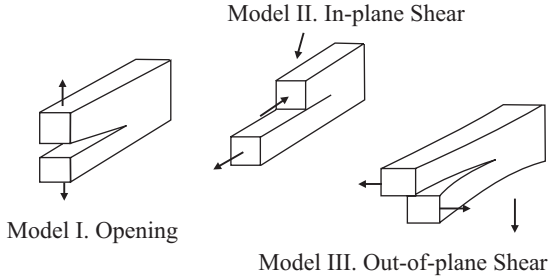

Fig. 3. Schematic depicting the various modes of fracture

The fracture toughness (K_{1c}) is computed using the correlation originally developed by Rolfe and Barsom [8] and recently reported by Chao et al [9]:

$$[K_{1c}/\sigma_{ys}]^2 = 5\ [\ CVN/\sigma_{ys} - 0.05] \quad (2)$$

Where K_{1c} is the fracture toughness at slow loading rates (ksi(in)$^{1/2}$), σ_{ys} is the 0.2% offset yield strength and CVN is the standard Charpy V-Notch impact test value. The yield point corresponds to the point where the material begins to have permanent deformation. The significance of the 0.2% offset point is that some materials have well-defined yield region, while others do not. In the absence of a distinct yield point, a 0.2% offset is used to obtain an approximate yield point. In this construction, a line originating at 0.2% strain is drawn parallel to the initial slope of the stress-strain curve. The intersection at the stress-strain curve defines the yield stress.

Optical microscopy

The fractured specimens were viewed under bright field monochromatic white light, using the Leica model DMLM (FRG) optical microscope. Sample preparation for the Ti-alloy followed the procedure, (a) wet cutting of the fractured portion to avoid temperature gradients and hot spots using tribological fluid, (a) mounting of the fractured surface on uncured epoxy resin, which is then cured at room temperature to hold the sample for grinding and polishing prior to viewing in the microscope. Sequential grinding involves placing the mounted surface against a spinning circular wheel employing SiC grinding media in the 80-2000 grit sizes. Polishing of the fractured surface was accomplished in two stages by applying 6 μ and 3 μ diamond paste on a polishing cloth mounted on a spinning wheel (320 rpm). The surface was finally etched by dipping in a solution of HF, HNO_3, H_2O, and two drops of H_2O_2 for 10 s.

Mechanical testing methods

The viscoelastic PU was studied with a Polymer Laboratories MkII Dynamic Mechanical Thermal Analyzer (PL-PMDTA). The storage and loss moduli and the loss tangent were obtained in the nominal temperature between –100 and 100°C and a frequency of 40 Hz. Data presented lay in the important glass transition and upper range. The specimens (typically 8 x 16 x 3 mm) were subjected to the bending mode of deformation.

UTM was performed on a software-configured Instron tensile tester at a crosshead speed of 50 mm min^{-1}. Standard dumbbell shaped specimens with gauge length of 50 mm and a gauge width of 10 mm were tested in an environmental chamber. The thickness of the samples was 3 mm, but varied slightly for the cast segmented PU where the thickness of the specimen was controlled by pouring the mixed PU to a pre-graduated casting tray. Stress-strain curves were obtained for both the cast PU and as received PU composite to determine the yield strength at break.

Micro-hardness testing was performed with a Shimadzu HMV-2T Micro-hardness Tester using a 300 g load over a period of 15 s (load application time). The tester has an automatic turret mechanism and once the impression is registered, the read button executes the hardness, which is displayed on the LCD screen. Vickers hardness values are reported in this paper.

Results and discussion

The microstructure of the Ti-6Al-4V alloy appears in Fig.4, which is akin to typical α-β titanium alloys. It compares well with the ASM standards, which shows that the alloy is forged and annealed [10]. The stabilizing β secondary phase is uniformly dispersed in the Ti matrix. The corresponding fractograph appears in Fig.5. Inter-crystalline, cup and cone fracture, typical of highly ductile materials is clearly demonstrated. This mimics in textbook fashion, the ductile fracture reported earlier for Al metal [11]. Extensive energy absorption leads to plastic deformation and work-hardening at the yield point as indicated by the measured micro-hardness in the yield zone close to the fracture tip and that in the base metal region. An increase in hardness to the tune of 45 Vickers units is observed close to the crack tip. The Ti-alloy fracture provides a baseline comparison with the viscoelastic PU counterparts used as interleaving layers in the armor kit.

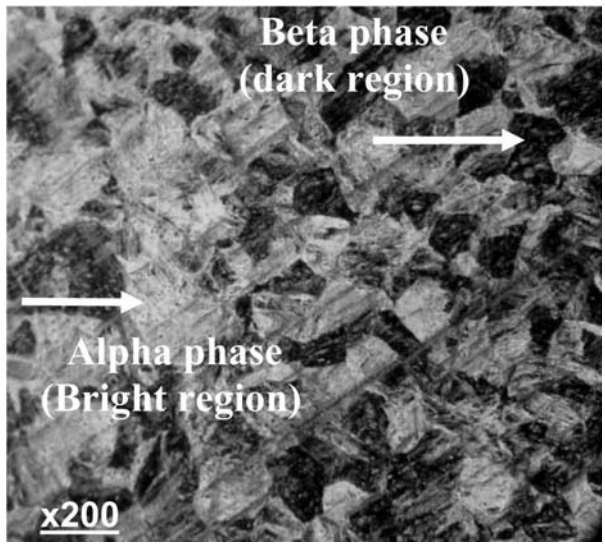

Fig. 4. Optical micrograph showing the microstructure of the Ti-6Al-4V alloy

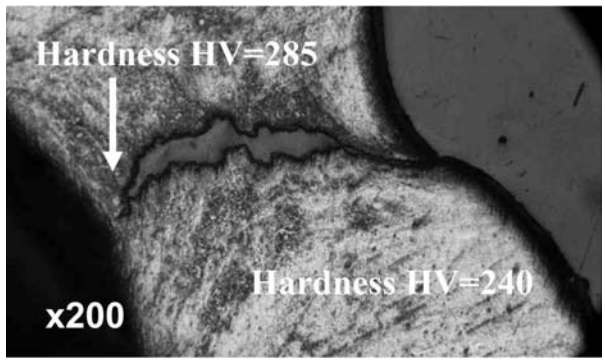

Fig. 5. Optical fractograph of the fractured Ti-6Al-4V alloy

Table 1 compares the impact energy and fracture toughness (K_{1c}) of the various materials studied. The two forms of granite exhibit similar fracture energies. Their fracture toughness is not listed owing to non-availability of the yield strength values. The fractographs obtained for the granites show plain cleavage type fracture attributed to brittle materials. The high impact energy arises from the secondary cracks that emanate from the primary cleavage zone. It is plausible that impact energy was dissipated via the formation of damage zones with a large number of micro-cracks in front of the main crack. Our experience with live rounds impacting a ceramic faceplate also shows that a deep-crevice facial buckling is accompanied by extensive multiple secondary crack growth leading to shattering, absorbing significant amount of energy on impact in the process.

Table I. Comparison of fracture energy and stress intensity factor for stand-alone and paired un-notched specimens of various materials

Specimen	Velocity m/s	Fracture Energy (J)	K_{1C} MN/m$^{1/2}$
Black Granite	5.04	174.9	-
Shaded Granite	5.04	181	-
PU Glass Composite	5.27	295	247
Segmented PU	5.06	No break	No break
Granite + PU Composite	5.00	182	152
Mild Steel	5.04	168	140
Mild Steel/PU Composite	5.04	178	148
Titanium	5.04	267.75	223

Both PU-glass composite and the segmented PU exhibitexceptional impact energy values. The PU composite is a polymer-filler system, which is basically heterogeneous. In this, the polymer is adsorbed at the surface of the filler particle through formation of hydrogen bonding or primary bonding and the nature of the adsorption layer are different from that of the original polymer phase. This mechanism is considered to be responsible for reinforcing effects such as an increase in modulus, which is an order of magnitude higher than the virgin PU (see later). As described earlier, composites based on polymers do have the ability to resist impact as they dissipate energy in the viscoelastic matrix and also absorb energy over a large surface being created as a result of dobonding at the polymer-filler interface.

In case of laminated structures i.e. when two material layers are used in conjunction, the results are instructive. As seen in Table 1, PU viscoelastic layers augment impact energy of ductile materials (Mn-steel), but do not complement the brittle ones (granites) so well. One possible reason for this behavior could be that the brittle materials fracture catastrophically, leaving very little opportunity for the viscolestic dampeners to absorb input energy. Elastomeric layers are thus best used in conjunction with ductile materials that offer considerable deformation before yielding. Although the segmented PU specimen did not fracture, it absorbed maximum permissible energy equivalent to the rated input of 300 J. The extraordinary energy absorption characteristics for this material are explained with reference to ATR-IR and DMTA scans of the polymer presented in Fig. 6, Fig. 7 and Fig. 8, Fig.9 respectively.

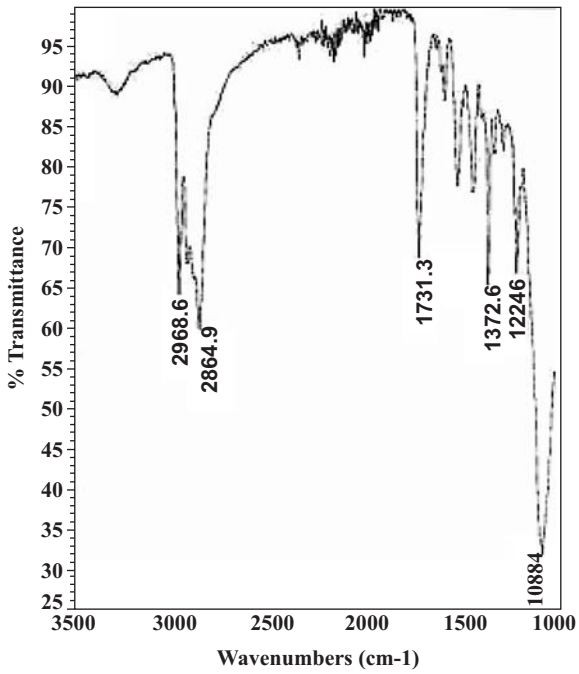

Fig. 6. ATR-IR of the cross-linked PU specimen

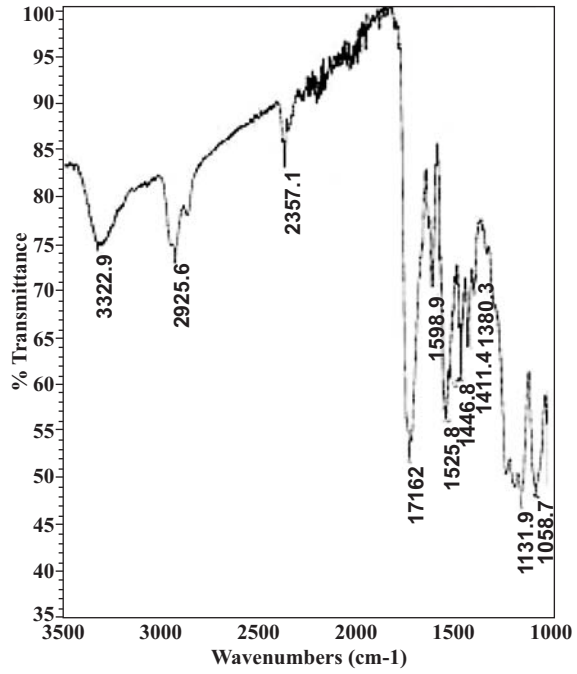

Fig. 7. ATR-IR of the segmented PU specimen

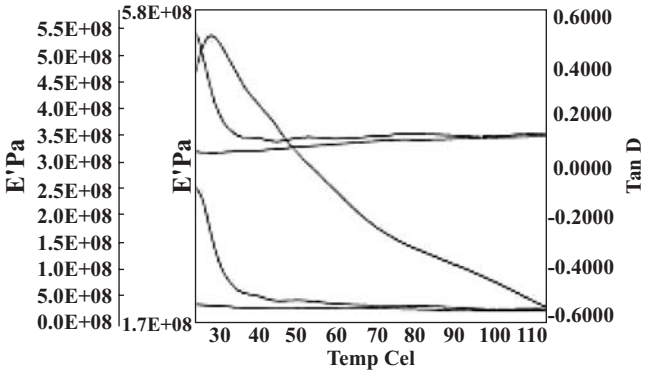

Fig. 8. DMTA of the cross-linked PU specimen

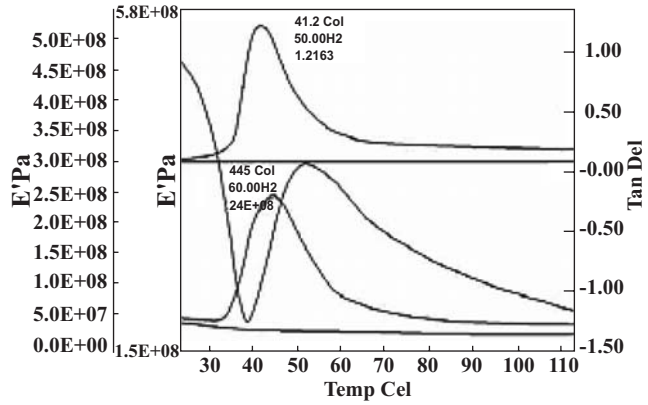

Fig. 9. DMTA of the segmented PU specimen

The ATR-IR spectra of the cross-linked and segmented polyurethanes are shown in Fig. 6 and Fig.7 respectively. The carbonyl (C=O) peak in the1730-1760 cm^{-1} represents the urethane (-NHCOO) group formed as a result of the diol/isocyanate reaction and is identical for both PU systems. However, a significant increase in the NH stretching peak is observed for the segmented PU. The NH stretching vibration is due to the NH---C=O hydrogen bonding among the urethane (-NHCOO) H^+ and carbonyl O^-as illustrated earlier for a similar system having different processing history [12]. Since both the functional groups participating in this vibration are associated with the hard segment, extensive phase separation has occurred in the segmented PU relative to its cross-linked counterpart (Fig.6).

It has been reported earlier that materials without chemical cross-links but with a high degree of hydrogen bonding in the hard domains, exhibit a large degree of stable crack growth with final failure occurring at higher ultimate deformation [13]. Likewise, it was observed that although hydrogen bonding gives some extra rigidity to the hard domains, they would have the ability to break and reform allowing more deformation of hard domains than chemical cross-links. This mechanism would lead to greater dissipation of energy within the polymer domains.

The DMTA scans for the segmented and cross-linked PU appear in Fig.8 and Fig.9, respectively. These scans show the storage (E') and loss modulus (E") as well as the loss tangent (E"/E'). The UTM curves for the PU-glass composite is also presented in Fig.10 for comparison of the tensile moduli of the virgin PU and its short fiber-doped composite. An order of magnitude increment in the modulus of the composite, as determined from the initial slope of the stress-strain curve, is observed. The DMTA scans were administered at a relatively high frequency of 40 Hz to simulate the impact test rate. Referring to Fig.8, a dual phase transition is observed for the micro-phase segregated PU E' curve, corresponding to the polyol soft segments and the BDO hard domains. In contradistinction, the cross-linked PU in Fig.9 reveals a single-phase transition. Furthermore, the loss tangent (1.21) of the segmented PU is far greater than that of the cross-linked one (0.60), albeit the storage modulus values for the two polymers are quite similar. The increased damping (greater E"/E' ratio) for the segmented PU specimen explains in substantial part the superior energy absorption obtained. An increased micro-phase separation normally narrows the E" transition peak [14]. A comparison of the E" peaks for the two polymers indicate that the breadth over which the relaxations contributing to the glass transitions occur is indeed greater for the cross-linked sample. The same effect (spreading of E" peak) has been found in the case of better inter-segment mixing achieved by heating the polymer [12].

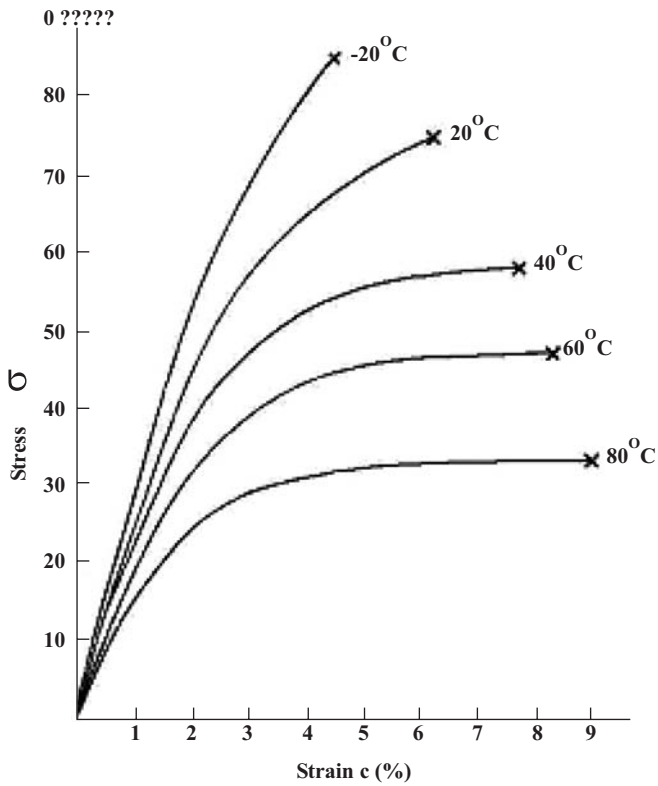

Fig. 10. UTM stress-strain curves for the glass fiber-doped PU composite

The observed impact response of the PU owes some explanation in terms of its nanostructure. Transmission electron microscopy (TEM) of the microtomed PU employing 50% hard segment (MDI-BDO) has been reported earlier [4], which shows lamellar domains that

form into fibrous, birefringent spherulites. There are, however, large regions where no structures can be observed indicating domains less than 10 nm. The latter are normally identified by wide angle X-ray scattering (WAXS). This featureless morphology seems to give ductile behavior, while the highly birefringent, spherulitic morphology seems to act, as reinforcement when the polymer is subjected to deformation, much like the particle-matrix composites. Similar behavior has been observed using polyterephthalate amorphous phase in conjunction with cyclobutane elastic phase [15].

The onset of the nano-segregation has been also assessed by ATR-IR. Fu et al [16] carried out IR spectroscopy for the entire three major polymer precursor chains i.e., polyester, polyether and polybutadiene and found phase-segregation as revealed by an enhanced –NH stretching peak at 3320 cm^{-1} together with a shift in the carbonyl peak at c.1750 cm^{-1} during polymerization. When urethane hard segments associate with each other, hydrogen bonds form between the carbonyl oxygen and the amine hydrogen. This results in the frequency shift in the C=O peak as observed. It is this association of hard segments that leads to the observed micro-phase segregation, which by and large determine the dynamic viscoelastic properties of the PU e.g., loss modulus and the damping coefficient, Tan δ.

Conclusion

The fracture toughness of a series of materials has been evaluated. Segmented polyurethane based on chain extension has been identified as a promising candidate for deployment as interleaving layers in composite armor kits. The advent of micro-phase segregation coupled with the accentuated loss modulus in this type of PU is mainly responsible for the extraordinary impact strength. The impact test data is well corroborated by the molecular spectroscopy and dynamic behavior analysis of the polymer. In case of the commodity glass-fiber PU composite, impact strength is augmented by the energy absorbed in fracturing the glass-fiber interface, which may be further improved by appropriate engineering of the polymer matrix along the lines suggested in the paper.

Acknowledgement

The author is grateful to Mr. Nadeem Ehsan of NSCME for his assistance in conducting impact tests and Mr. T. Sultan of the National Development Complex for preparation of the specimens for optical microscopy.

REFERENCES

1. C. Visconti, G. Caprino, R. Teti, and F. Langella, “Composite materials under impact conditions”, *First European Conference on Composite Materials*, France 1985, pp. 228.
2. R. Baily and M. G. Bader, “The effect of toughening on the fracture behavior of glass reinforced polyamide”, *First European Conference on Composite materials*, France 1985, pp. 265.
3. M. B. Khan, *Handbook of Engineering Polymeric Materials*, N. P. Cheremissinof, ed. 1997, N.Y: Marcel Dekker, pp. 705-724.
4. C. P. Christenson, M. A. Harthcock, M. D. Meadows, H. L. Spell, W. L. Howard, M. W. Creswick , R. E. Guerra and R. B. Turner, “Model MDI/Butanediol polyurethanes: Molecular structure, morphology, physical and mechanical properties”, *J. Polym. Sci: Part B. Phys*., Vol. 24, 1986, pp. 1401-1439.
5. W. F. Smith, *Structure and Properties of Engineering Alloys*, 2nd ed. N.Y./London: McGraw Hill, 1993, pp. 472.
6. M. B. Khan, “SEM comparison of traditional and modulus gradient-induced particulate composites of polyurethane nano-polymer”, *The Nucleus*, 2007, Vol. 44, No. 3-4, pp. 105-110.
7. N. J. Harrick, *Internal Reflection Spectroscopy*, N.Y: Wiley, 1987, pp.30.
8. J. M. Barsom and S. T. Rolfe, *Fracture and Fatigue Control in Structures*, Englewood Cliffs, NJ: Prentice-Hall, Inc. 1987.
9. Y. J. Chao, J. D. Ward, and R. G. Sands, “Charpy impact energy, fracture toughness and ductile–brittle transition temperature of dual-phase 590 Steel”, *Materials & Design*, Vol. 28, No. 2, 2007, pp. 551-557.
10. *ASM Metallography and Microstructures Handbook,* 9th ed. Vol. 9, 1998, pp.469
11. H. W. Hayden, W. G. Moffet and J. Wulff, *The Structure and Properties of Materials*, Vol. 3, Mechanical Behavior, N.Y. Wiley, 1965, pp.144
12. B. J. Briscoe, M. B. Khan and S. M. Richardson, “Adhesion modification by shear-enhanced localized interfacial segregation in model reaction injection molded (RIM) polyurethanes”, *J. Adhesion Sci. Technol*, 1989, 3:6, pp. 475-497.
13. R. A. Beck and R. W. Truss, “The effect of stoichiometry on the fracture toughness of a polyurethane-urea elastomer”, *Polymer*, Vol. 40, 1999, pp. 307-313.
14. L. E. Nielsen, *Mechanical Properties of Polymers and Composites*, Marcel Dekker, N.Y: 1994.
15. C. J. Booth, M. Kindinger, H. R. McKenzie, J. Hancock, A.V. Bray and Beall GW. “Copolyterephthalates containing tetra-methylcyclobutane with impact and ballistic properties greater than bisphenol: a polycarbonate”, *Polymer.* Vol. 47 2006, pp. 6398-6405.
16. B. Fu, W. J. Macknight and N. S. Schneider, *Rubb. Chem. & Technol*, Vol. 69, 1987, pp. 896.